



Orijinal Araştırma / Original Research

## TECHNOLOGICAL CHARACTERIZATION AND COMPARISON OF TWO CERAMIC CLAYS USED FOR MANUFACTURING OF TRADITIONAL CERAMIC PRODUCTS IN TURKEY

### TÜRKİYE'DE GELENEKSEL SERAMİK ÜRÜNLERİN İMALATINDA KULLANILAN İKİ SERAMİK KİLİNİN TEKNOLOJİK TANIMLAMASI VE KARŞILAŞTIRILMASI

Haluk Çelik<sup>a,\*</sup>

<sup>a</sup> Uşak Üniversitesi, Mühendislik Fakültesi, Maden Mühendisliği Bölümü, UŞAK

Geliş Tarihi / Received : 8 Haziran / June 2017

Kabul Tarihi / Accepted : 2 Ekim / October 2017

#### Keywords:

Clay,  
Ceramic,  
Ceramic mud,  
Drying sensitivity index

#### ABSTRACT

In the present investigation, two different clay samples from the region of Menemen (İzmir) and the region of Kınık (Bilecik) were characterized by mineralogical, chemical and thermal analyses and different technological tests. The drying sensitivity of the clay bodies was also studied by determining Drying Sensitivity Index. The results revealed that the Menemen Clay (MC) composed of kaolinite and muscovite clay minerals whereas Kınık Clay (KC) consists mostly of clinocllore and muscovite. The MC contains about 50% clay minerals and 35.71% quartz whereas the KC has about 41% clay minerals and 50% quartz. As a result of this composition, the firing shrinkage and total shrinkage values of the MC were higher than that of the KC. On the other hand, the KC presents a higher value of plasticity index (PI) than the MC. On the evaluation of drying sensitivity of two ceramic muds, it was concluded that the KC has the less Drying Sensitivity Index (DSI) (0.75) value than the MC (0.84).

#### ÖZ

Bu çalışmada, Menemen (İzmir) ve Kınık (Bilecik) bölgelerinden alınan iki farklı kil numunesinin mineralojik, kimyasal, ısıl ve teknolojik özellikleri belirlenerek tanımlaması yapılmıştır. Kil bünyelerinin kuruma hassasiyeti Kuruma Hassasiyeti İndeksi belirlenmek suretiyle çalışılmıştır. Sonuçlara göre Menemen Kili (MC) kaolinit ve muskovit minerallerinden oluşmakta iken, Kınık Kili (KC) çoğunlukla klinoklor ve muskovit içermektedir. MC %50 kil mineralleri ve %35.71 kuvars içerirken, KC %41 kil mineralleri ve %50 kuvars içeriğine sahiptir. Bunun bir sonucu olarak MC'nin pişirme küçülmesi ve toplam küçülme değerleri KC'den daha yüksek çıkmıştır. Diğer taraftan KC'nin plastisite indeksi (PI) MC'den daha yüksektir. İki seramik çamurunun kuruma hassasiyetlerinin değerlendirilmesi neticesinde KC'nin (0.75) MC'den (0.84) daha düşük Kuruma Hassasiyeti İndeksi (DSI) değerine sahip olduğu sonucuna ulaşılmıştır.

#### Anahtar Sözcükler:

Kil,  
Seramik,  
Seramik çamuru,  
Kuruma hassasiyeti indeksi.

\* Sorumlu yazar: [haluk.celik@usak.edu.tr](mailto:haluk.celik@usak.edu.tr) • <https://orcid.org/0000-0002-9964-1566>

## INTRODUCTION

Clays and clay minerals used in various process industries are crucial industrial minerals (Harvey and Murray, 2006). Clay minerals are the main constituents for traditional ceramic industries and some advanced ceramic products. Application of clay minerals in these industries depends on their chemical compositions, mineralogy, and physical properties. The small size of the particles and their unique crystal structures give clay materials special properties, including cation exchange capabilities, plastic behaviour when wet, catalytic abilities, swelling behaviour, and low permeability. Clays undergo a lot of physical and chemical changes with various firing temperatures, which, in turn, predominantly determine their ceramic properties and their uses as an industrial ceramic raw material (Baccour et al., 2009; Carretero et al., 2002; Celik, 2010; Ozkan, 2015).

In Menemen (İzmir, Aegean region of Turkey) and in Kınık (Bilecik, Marmara region of Turkey), there are extensive clay deposits, the clay from which are fired in different colours. These clays are currently being used by local ceramic manufacturers for traditional pottery and brick production. Hence, these two regions remain important pottery centres of Turkey.

The aim of this study is to determine the technological characterisation and comparison of Menemen Clay (MC) and Kınık Clay (KC). For this purpose, the clay samples were first characterized by chemical analyses, X-ray diffraction (XRD) analyses and plasticity measurements, etc. Subsequently, the Drying Sensitivity Index of ceramic mud was determined by employing the Bigot's method. It is expected that the present investigation will help to improve the resourcefulness of the knowledge on the Menemen Clay and Kınık Clay. Although limited characterisation studies of red firing MC have been reported in the existing literature on this field of study (Ozkan 2015; Colak and Aksu, 2001), characterisation of the KC and the comparison of these deposits have not been studied comprehensively before.

## 1. MATERIALS AND METHODS

### 1.1. Sample Material

The MC deposit is located about 35 km north of İzmir, whereas the KC deposit is located near to the town of Pazaryeri, about 36km south of the Bilecik City. These deposits are widely used as raw materials by ceramic manufacturers in Turkey for

the production of earthenware ceramics, i.e. traditional pottery and brick production. Five bag samples (20 kg each) were supplied from the ceramic manufacturers for the MC and the KC. They were blended, quartered into about 1 kg of specimens for laboratory assessment including characterization study and industrial processing tests.

### 1.2. Mineralogical and Chemical Analyses

The mineralogical characterization of the samples was carried out by XRD analyses. The XRD patterns were obtained with a Rigaku Rint-2200 diffractometer operating at tube voltage and current 40 kV and 30 mA, respectively using monochromatic Cu-K $\alpha$ 1 radiation ( $\lambda=1.5406 \text{ \AA}$ ). Diffraction patterns were recorded between  $5^\circ$  and  $70^\circ(2\theta)$  with a scanning rate of  $2^\circ/\text{min}$ . Quantification of different phases in the samples was carried out using the computer program MAUD 1.9 (Lutterotti, 2010), which is based upon the Rietveld method combined with a Fourier analyses (Can et al., 2010). Phase changes of fired samples at  $1000^\circ\text{C}$  of the MC and the KC were also investigated by XRD method. The chemical compositions of raw materials were determined using X-ray fluorescence spectroscopy (XRF, Rigaku ZSX Primus).

### 1.3. Thermal Analyses (DTA-TGA and Dilatometry Tests and Thermal Expansion Coefficients)

Differential thermal analyses-thermo gravimetric analyses (DTA-TGA) of the samples were determined by a differential calorimeter apparatus (Netzsch STA 409) under air atmosphere. The temperature was increased from room temperature to  $1200^\circ\text{C}$  at a rate of  $10^\circ\text{C}/\text{min}$ , and it was kept at this maximum temperature for 10 minutes.

The firing characteristics of the raw clay samples were determined by heating the sample up to  $1250^\circ\text{C}$  at a heating rate of  $50^\circ\text{C}/\text{min}$  for  $<1100^\circ\text{C}$  and  $30^\circ\text{C}/\text{min}$  for  $1100\text{-}1250^\circ\text{C}$  and maintained at the maximum temperature for 10 minutes. The pressed sample was dried overnight at  $105^\circ\text{C}$  and then heated in Misura 3.32 ODHT-HSM 1600/80 dilatometer. Length changes were recorded at every minute during the heating stage.

The thermal expansion coefficients of the selected samples of dimensions  $25\text{mm}\times 5\text{mm}\times 5\text{mm}$  were also determined using a computer-controlled Netzsch thermal dilatometer (Model: 402 EP) at a heating rate of  $10^\circ\text{C}/\text{min}$  to  $650^\circ\text{C}$ .

#### 1.4. Particle Size Analyses

A combination of wet sieving for the fraction  $>63\mu\text{m}$  and X-ray sedimentation technique for the fraction  $<63\mu\text{m}$  was used. For the sieving, 100 grams of samples dispersed in deionized water were disaggregated using 0.1% sodium hexametaphosphate (SHMP) ( $\text{Na}_6\text{O}_{18}\text{P}_6$ ). For the X-ray sedimentation analyses, the  $<63\mu\text{m}$  fraction (about 3 grams) was disaggregated using 0.5% SHMP, agitated mechanically and disaggregated ultrasonically. The size analyses were performed with the Mikromeritics SediGraph 5120 particle size analyzer, at a size range between 0.1–300 $\mu\text{m}$ .

#### 1.5. Industrial Tests

Rectangular samples in dimensions of 84mm $\times$ 20mm $\times$ 7mm for bending strength measurements and cylinders samples in dimensions of 50mm $\times$ 6mm for determination of shrinkage and water absorption rate were uniaxially pressed by a standard laboratory hydraulic press (Gabbrielli Titan, Italy mark) at 250kg/cm<sup>2</sup>. First of all, the specimens were kept in a room prevented from the air flow until the weight became constant for determination of drying shrinkage (DS) and mass loss. Then, the representative tiles were fired in a laboratory electric furnace at a peak temperature of 1000°C (soaking time 8 minutes). In order to obtain gresification diagram of the fired samples of the MC and the KC, the specimens were sintered in a laboratory electric furnace at the temperature between 900-1200°C.

The technological properties of the representative samples fired at 1000°C like water absorption and bending strength were measured in accordance with the Turkish standards procedures (TS EN ISO 10545-3, 1995; TS EN ISO 10545-4, 1995). On average, ten specimens were used for each measurement. The bending strength (BS) values were determined by a three-point bending test using a Universal Testing Machine (Nannetti Faenza, Italy), and calculated by  $3FL/2bh^2$  in which F=breaking load (kg), L=distance between supports (mm), b=sample width (mm) and h=sample thickness (mm). The support span of 80 mm and the crosshead speed of 5 mm/min were chosen for all measurements. The water absorption values ( $W_a\%$ ) were determined by the routine procedure involving measuring mass differences between the as-fired (D) and water saturated samples (M) (immersed in boiling water for 2h, cooling for 3h and sweeping of their surface with

a wet towel) using  $100(M-D)/D$  equation. The dimensions of the pressed specimens were measured before and after firing to determine the firing shrinkage (FS%) by  $100(L_d-L_f)/L_d$ , where  $L_d$ =the length of the dried specimen and  $L_f$ =the length of the fired specimen. The total shrinkage (TS%) was calculated by  $100(L_i-L_f)/L_i$ , where  $L_i$ =the initial diameter of the cylindrical specimen (50mm).

#### 1.6. Evaluation of Plasticity

The evaluation of plasticity was performed by Atterberg limits method: liquid limit (LL), plastic limit (PL) and plasticity index (PI). The plasticity index was calculated based on the arithmetic difference of the LL and PL of the studied clays. LL and PL tests were carried out with a Casagrande apparatus using the method described by Casagrande (1947).

#### 1.7. Drying Sensitivity Measurement

Drying of ceramics is understood as a process of removing water from an unfired ceramic object or raw material in the green or as formed state. It is a complex process involving simultaneous heat and mass transfer between the body and a surrounding atmosphere (Aungatichart and Wada, 2009). Drying sensitivity is one of the good indicators to evaluate the easiness of drying. There are many papers related to the drying sensitivity of clay materials (Aungatichart and Wada, 2009; Atanasov, 2005; Ratzenberger, 1986a; Ratzenberger, 1986b; Ratzenberger, 1990; Reinholz, 1987; Schneider and Hanke, 1996). Bigot's curve method was used to determine Drying Sensitivity Index (DSI) as described in the literature (Aungatichart and Wada, 2009). Specimen preparation and measurement methods for the DSI are as follows:

- (I) The plastic dough was formed into a rectangular bar of 120 $\times$ 20 $\times$ 5 mm in size.
- (II) The specimen was put on a glass plate with a thin paper lining. The paper would shrink with the specimen during drying.
- (III) On the top surface of the specimen, 100 mm distance was marked.
- (IV) The specimen was kept in a room prevented from the air flow for 48 h.
- (V) The weight of the specimen together with the glass and the paper was taken, and the length of the mark on the specimen was also measured at 0, 1, 2, 3,... until 48 h.

(VI) The specimen was dried at 110°C until the weight became constant (24 h) and the length of the dried specimen was measured in order to calculate the drying shrinkage (DS).

(VII) The graph of the relationship between shrinkage and water content was plotted.

(VIII) The DSI was calculated using the equation  $DSI = ((M_i - M_c)/100) \times DS$ . Where;

-DSI: Drying Sensitivity Index

- $M_i$ : the initial moisture of the dough (%)

- $M_c$ : the critical moisture at which the drying shrinkage finishes (%)

-DS: drying shrinkage of specimens dried at 110°C for 24h (%)

## 2. RESULTS AND DISCUSSION

### 2.1. Mineralogical and Chemical Analyses

Fig. 1 shows the XRD patterns of the clay samples. The following mineralogical phases were identified for the MC; kaolinite ( $Al_2O_3 \cdot 2SiO_2 \cdot 2H_2O$ ) (JCPDS Card No:029-1488), albite ( $Na_2O \cdot Al_2O_3 \cdot 6SiO_2$ ) (JCPDS Card No:009-0466), calcite ( $CaCO_3$ ) (JCPDS Card No:047-1743), muscovite ( $KAl_2(Si_3Al)O_{10}(OH)_2$ ) a member of mica group clay minerals (JCPDS Card No:007-0042) and quartz ( $SiO_2$ ) (JCPDS Card No:046-1045), whereas the KC consists mostly of clinocllore ( $Mg_5Al(AlSi_3O_{10})(OH)_8$ ) (JCPDS Card No:024-0506), which is a member of chlorite group clay minerals (Bergaya and Lagaly, 2006), albite (JCPDS Card No:009-0466), muscovite (JCPDS Card No:007-0042) and quartz (JCPDS Card No:046-1045).

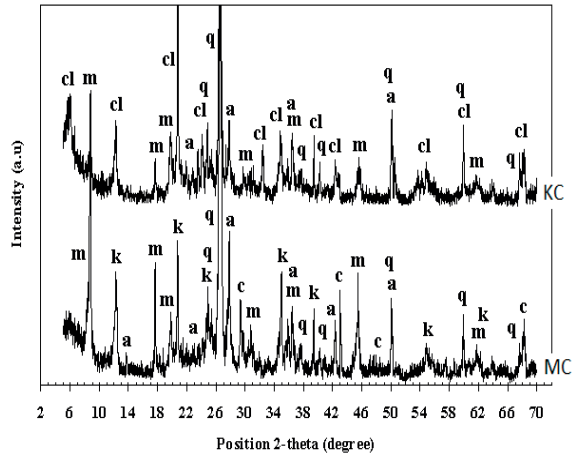


Figure 1. X-ray diffraction patterns of the raw samples MC, and KC (cl:clinocllore, a:albite, m:muscovite, k:kaolinite, c:calcite, q:quartz)

The crystalline phases identified are in agreement with the results observed by XRF (Table 1). The two clays consist mainly of  $SiO_2$  and  $Al_2O_3$  which correspond to about 70% for the MC and 72% for the KC as shown in Table 1, because of the presence of clay minerals and quartz and accompanied by albite for the MC and the KC.

It is considered that the KC has relatively more quartz and less clay mineral than the MC, in consequence of higher  $SiO_2/Al_2O_3$  ratio for the KC (3.32) than for the MC (2.98). Coherent with the XRF results, the MC contains about 50% clay minerals and 35.71% quartz whereas the KC has about 41% clay minerals and 50% quartz as shown in Table 2.

The amount of alkaline oxides ( $K_2O$  and  $Na_2O$ ) that act as flux materials of the MC (4.39%) is

Table 1. Chemical compositions (mass%) of the clay materials

|    | $SiO_2$ | $Al_2O_3$ | $Fe_2O_3$ | $TiO_2$ | CaO  | MgO  | $Na_2O$ | $K_2O$ | MnO  | $P_2O_5$ | $Cr_2O_3$ | LOI*  |
|----|---------|-----------|-----------|---------|------|------|---------|--------|------|----------|-----------|-------|
| MC | 52.66   | 17.67     | 6.70      | 0.91    | 4.77 | 2.17 | 0.98    | 3.41   | 0.09 | 0.11     | 0.08      | 10.44 |
| KC | 55.62   | 16.73     | 7.64      | 1.14    | 1.36 | 3.74 | 1.00    | 2.38   | 0.15 | 0.12     | 0.09      | 10.03 |

\*LOI=loss on ignition (10°C/min up to 1000°C, and maintained at this maximum temperature for 1 h)

Table 2. Mineral content of the raw clay samples estimated by the computer program MAUD 1.9

|    | Kaolinite  | Muscovite  | Albite    | Quartz     | Calcite   | Clinocllore |
|----|------------|------------|-----------|------------|-----------|-------------|
| MC | 13.04±0.62 | 36.91±0.85 | 9.85±0.86 | 35.71±0.54 | 4.49±0.24 | ---         |
| KC | ---        | 19.76±0.92 | 8.89±0.24 | 49.91±0.68 | ---       | 21.42±0.36  |

higher than the KC (3.38%) probably due to a relatively large amount of muscovite content. In clay based bodies, flux materials enable to lower the temperature which liquid or glass forms during sintering. The amounts of earth-alkaline (CaO and MgO) oxides are 6.94% and 5.1% for the MC, and the KC respectively coherent with the XRD results. The MC contains a carbonate mineral (calcite). The  $Fe_2O_3$  content of the MC is on the lower side when compared with the KC.  $Fe_2O_3$  is not the only factor responsible for the coloration of ceramic wares, as also other constituents such as CaO, MgO, MnO and  $TiO_2$  can appreciably modify the color of fired clay (Kreimeyer, 1987). Moreover, the temperature of firing, the amount of  $Al_2O_3$  relative to a range of other constituents, and the furnace atmosphere all play an important role in the development of color in the fired clay products (Fisher, 1984).

Typical XRD patterns of fired raw clay samples at 1000°C are given in Fig. 2. An overall examination shows that kaolinite and muscovite clay minerals and calcite existing in the MC disappeared firing at 1000°C, while andradite ( $Ca_3Fe_2(SiO_4)_3$ ) (JCPDS Card No:010-0288) appeared as new crystalline phases probably due to the reaction between disappeared minerals. Even if the minimum melting point of muscovite is 1130°C, it was lowered to 1000 °C because of the effect of other components such as calcite (Diels and Jaeckel, 2013). The clinocllore and albite minerals existing in the KC disappeared while the anorthite ( $CaAl_2Si_2O_8$ ) (JCPDS Card No: 018-1202) and sekaninaite ( $Fe_2Al_4Si_5O_{18}$ ) (JCPDS Card No: 031-0616) appeared as new crystalline phases.

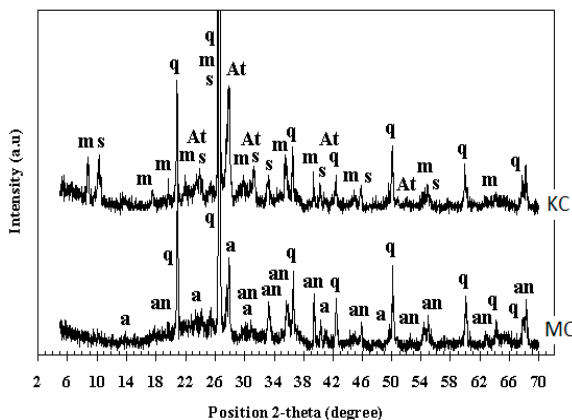


Figure 2. X-ray diffraction patterns of fired (at 1000°C) MC, and KC (s:sekaninaite, a:albite, m:muscovite, At:anorthite, q:quartz, an:andradite)

## 2.2. Thermal Analyses (DTA-TGA and Dilatometry Tests and Thermal Expansion Coefficients)

The interpretation of the DTA-TGA curves of the MC (Fig. 3) and the KC (Fig. 4) leads to the following results:

A significant endothermic peak at 109°C for the MC and 125°C for the KC can be attributed to the removal of adsorbed and interlayer water of clay minerals. The mass loss associated with this peak is about 1% for the MC and the KC. In addition, a large exothermic event until the peak point of 350°C and 300°C for the MC and the KC, respectively due to organic matter decomposition was observed for both studied clays.

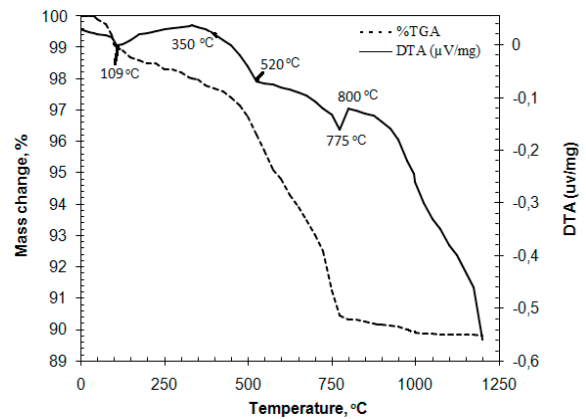


Figure 3. DTA and TGA curves of the MC

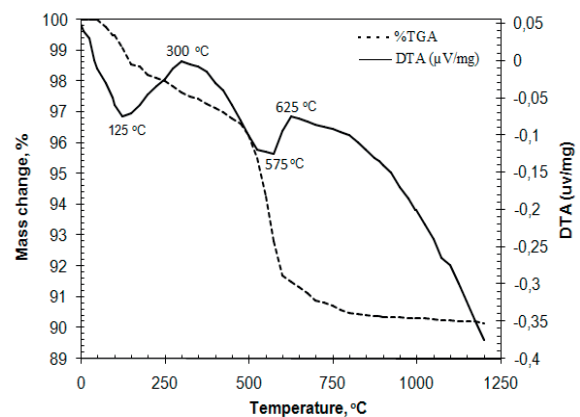


Figure 4. DTA and TGA curves of the KC

A broad endothermic band centered at 520°C for the MC and 575°C for the KC is due to both clay minerals dehydroxylation (for kaolinite dehydroxylation leading to the formation of metakaolinite) and  $\alpha \rightarrow \beta$ -quartz transformation. The MC (about

3%) undergoes the mass loss associated to this endothermic peak (about 4% for the KC). The dehydroxylation stage has important consequences for the stability of fired bodies because water molecules evaporate during the dehydroxylation stage and subsequently the structure of clay minerals collapses. The small endothermic peak at 775°C for the MC can be attributed to the calcite decomposition coherent with the XRD result. An exothermic peak was obtained at 800°C and 625°C for the MC and the KC, respectively. The appearance of these exothermic peaks is due to the formation of new crystalline phases. The total loss in weight after running DTA/TGA to 1200°C was about 10% for both samples, consistent with the loss on ignition value at Table 1. It is noted that the thermal behaviors of the clay samples are coherent with their chemical and mineralogical compositions.

The dimensional changes observed after firing of the raw clays are given in Fig. 5.

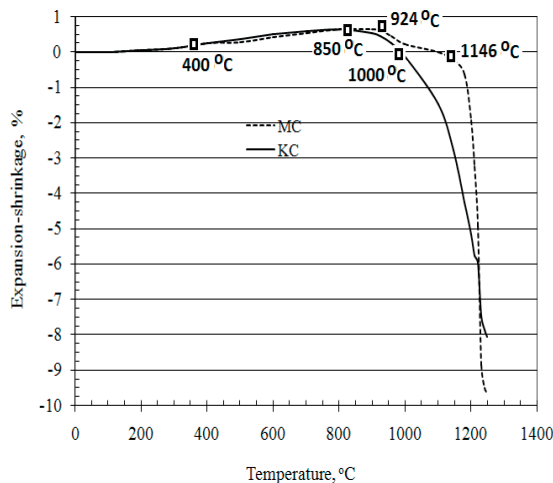


Figure 5. Dilatometric curves of the MC and the KC

It can be observed from the MC curve that there is a small expansion (0.25%) up to 400°C followed by more expansion between 400-924°C due to polymorphic  $\alpha \rightarrow \beta$ -quartz transformation,  $\beta$ -quartz  $\rightarrow \beta 2$ -tridymite transformation and due to metakaolinite formation with concomitant loss of water as suggested previously by Souza et al. (2002). Singer and Singer (1963) point out that  $\alpha$ -quartz transforms  $\beta$ -quartz at 573°C with a volume increase of 2% and on further slow heating  $\beta$ -quartz changes to  $\beta 2$ -tridymite at 870°C with a volume increase of 12%. The total expansion up to 924°C is 0.6%. After a slight shrinkage starting

at around 924°C, a sharp shrinkage starting at 1000°C is attributed to particles sintering and the formation of vitreous phases. The greatest shrinkage speed between 924-1146°C is obtained at 1000°C. When the temperature reaches the maximum point (1250°C), the shrinkage rate is about 10%. The total shrinkage after the temperature reduced to room temperature is 8.74%.

As it can be noticed, the dilatometric curve of the KC starts with the slight expansion up to 400°C similar to the MC, which can be attributed to the diminution of the adsorbed water. The second expansion between 400-850°C may be due to quartz transformation as described above. The total expansion up to 850°C is 0.6%. The slight shrinkage between 850-1000°C can be attributed to particles sintering and the formation of vitreous phases. The second shrinkage seen above 1000°C seems to be due to the recrystallization of new ceramic phases and vitrification. The maximum shrinkage speed above 1000°C is obtained at 1070°C. The total shrinkage after the temperature reduced to room temperature is assigned as 7.73%.

The obtained dilatometric results demonstrate that the MC, which possesses a larger quantity of clay minerals as stated from the result of particle size analyses and the quantitative XRD analyses, show more firing shrinkage compared with the KC. At the same time, it can be said that the relatively low rate of shrinkage of the KC indicates more content of quartz mineral than MC coherent with the XRD and the XRF results.

The results of linear thermal expansion coefficient's values of the clay bodies for a specific temperature range are also reported in Table 3. It is clear from Table 3 that the thermal expansion of the MC body is slightly lower than that of the KC. This is expected since there appears to be a higher amount of glassy phase in the MC body which dissolves more free quartz into the melt (Celik, 2015; Kurama et al., 2007).

### 2.3. Particle Size Analyses

The particle size distribution of clay is a factor in determining its suitability for various applications, and particular attention should be given to the finer fraction (lower than  $<2\mu\text{m}$ ) for ceramic products (Mahmoudi et al., 2008). Fig. 6 shows the cumulative results of particle size analyses of the clay samples. The KC presents a wider particle size distribution range, with an average particle size of about 50  $\mu\text{m}$  with 80% mass while

the average particle size of the MC is about 15  $\mu\text{m}$ . It can be observed that the percentage of clay minerals (particles with sizes  $<2\mu\text{m}$ ) is about 46% for the MC, whereas it is 40% for the KC. The silt fractions (particles with sizes between 2 and  $20\mu\text{m}$ ) are about 38% for the MC and 30.18% for the KC. The sand fraction (particles with sizes  $>20\mu\text{m}$ ) is about 16% for the MC and 29.42% for the KC (see Table 4). Particle size analyses results are coherent with the qualitative analyses of the samples. As calculated from Table 2, clay minerals content of the MC is about 50% whereas it is 41% for the KC.

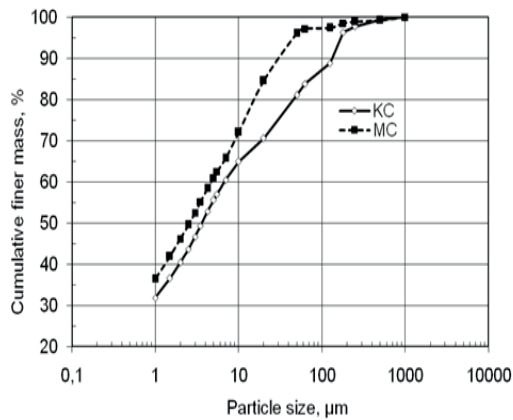


Figure 6. Particle size distribution of the MC and the KC

### 2.4. Industrial Tests

The results of the physical parameters obtained from industrial tests of the MC and the KC are shown in Table 3. The drying shrinkage value of the MC was 7.6% whereas the KC was 5.4%. In the drying step, it is adequate to obtain a value of drying shrinkage between 0-0.5% in order to avoid microcracks around sand grains (Baccour et al., 2008). The both samples had almost the same properties in drying bending strength. The water absorption increases slightly from 5.77% for the MC to 7.31% for the KC as shown in Table 3. Coherent with the  $W_a\%$  values, the firing bending strength increases 162  $\text{N/mm}^2$  for the KC to 179  $\text{N/mm}^2$  for the MC. The firing shrinkage and total shrinkage values of the MC were higher than the KC as shown in Table 3. This may be due to the presence of more quartz in the KC and more clay and more alkaline oxide content ( $\text{K}_2\text{O}$  and  $\text{Na}_2\text{O}$ ) in the MC coherent with the chemical analyses. It is recognized that reducing the content of clay in the KC causes a decrease in bending strength.

The sintering behavior of the clay samples was evaluated by using gresification diagrams (Figs. 7 and 8), which present the variation in properties of a ceramic as a function of firing temperature. As seen from Figs. 7 and 8, above  $950^\circ\text{C}$ , the values of water absorption decrease distinctly, as it

Table 3. Drying and firing characteristics and drying sensitivity characteristics of MC and KC samples

|   |   | MC*   | KC*   |
|---|---|-------|-------|
| Drying characteristics                              | Bending strength, BS, $\text{N/mm}^2$                                   | 11.1  | 10.8  |
|   | Shrinkage, DS, %  | 7.6   | 5.4   |
|   | Water absorption, $W_a\%$   | 5.77  | 7.31  |
| Firing characteristics (1000°C)                     | Bending strength, BS, $\text{N/mm}^2$                                   | 179   | 162   |
|   | Shrinkage, FS, %  | 10.82 | 9.51  |
|   | Total shrinkage, TS, %  | 17.60 | 14.40 |
| Drying sensitivity characteristics (Bigot's method) | The initial moisture of the dough, $M_i$ (%)                            | 23.45 | 21.59 |
|   | The critical moisture at which the drying shrinkage finishes, $M_c$ (%) | 11.41 | 6.53  |
|   | Drying shrinkage of specimens dried at $110^\circ\text{C}$ , DS (%)     | 7.00  | 5.00  |
|   | DSI: Drying Sensitivity Index   | 0.84  | 0.75  |
| Thermal expansion coefficients                      | $10^{-7}/^\circ\text{C}$ (20–400°C)                                     | 64.2  | 66.5  |

\*average of ten specimens

is associated to a more significant liquid phase formation. This phase penetrates the pores, closing them and isolating neighboring pores.

The liquid surface tension and capillarity help to bring pores closer together and reduce porosity; this explains the intense decrease of the water absorption in this temperature range (Baccour et al., 2009). The firing shrinkage up to 950°C is around 9% for the MC and 7.25% for the KC. Above 950°C, the firing shrinkage increases progressively to 13% for the MC while to 14% for the KC at 1200°C. The firing temperature has an important effect on the mechanical strength of ceramic tile. The bending strength of the MC increased progressively from 134 to 152, 179, 186, 192, 195 and 208 N/mm<sup>2</sup> fired at temperature displayed at Fig. 7, respectively. The mentioned values for the KC were 125, 144, 162, 181, 199, 206 and 211 N/mm<sup>2</sup>. The effect of the temperature was to increase the bending strength by means of densification. As mentioned before, liquid phase formation above 950°C reduces porosity, which hinders crack formation and improves the mechanical strength.

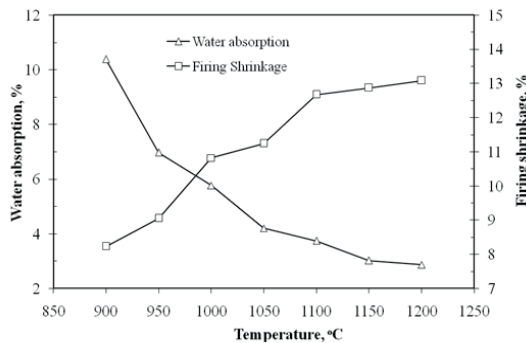


Figure 7. Gresification diagram of fired samples of the MC

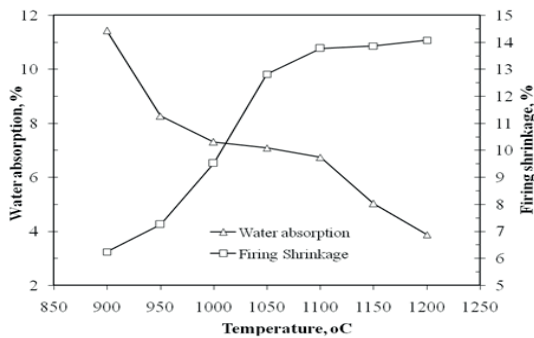


Figure 8. Gresification diagram of fired samples of the KC

## 2.5. Evaluation of Plasticity

The mineralogical composition of distinct argillaceous materials can influence their plasticity. The clay mineral fraction, clay minerals types, the quantity and type of natural accessory materials can alter plasticity (Modesto and Bernardin, 2008). Among the main impurities that possess non-plastic properties are iron minerals (mainly Fe<sub>2</sub>O<sub>3</sub>), aluminum oxide, sodic and potassium feldspars, soluble salts (K<sub>2</sub>SO<sub>4</sub>, NaCl, Na<sub>2</sub>CO<sub>3</sub>, etc.), calcium minerals (mainly calcite) and silica (Ancy, 2007; Peters, 1991). Table 4 depicts the results of the plasticity tests, given by the Atterberg limits. One may observe that the KC presents a higher value of plasticity index (PI) than the MC. In fact, the elevated values of PI characterize them as highly plastic, which is also demonstrated by Casagrande diagram (Casagrande, 1947) (Fig. 9) based on given data in Table 4.

Table 4. Fractional particle size distribution and Atterberg parameters of the clay materials

|                             | MC     | KC     |
|-----------------------------|--------|--------|
| Liquid limit, LL, mass%     | 58.1   | 62.3   |
| Plastic limit, PL, mass%    | 23.8   | 21.7   |
| Plasticity index, PI, mass% | 34.3   | 40.6   |
| >2000 µm                    | -      | -      |
| 200-2000 µm                 | 2.00   | 3.00   |
| 20-200 µm                   | 13.41  | 26.42  |
| 2-20 µm                     | 38.45  | 30.18  |
| <2 µm                       | 46.14  | 40.40  |
| Total                       | 100.00 | 100.00 |

Because the MC has more amount of clay fraction (<2µm) as indicating from particle size analyses, the MC has more plastic limit (PL) than the KC. The plasticity parameters of the MC are quite similar to results of the study (Ozkan, 2015). Both the MC and the KC samples also show high values for the PL, which has an important technological application, since it indicates the minimum percentage of moisture necessary to reach a plastic condition. With a high plastic limit, there will be more difficulty in drying the samples. On the other hand, the use of high plastic clays contributes to a reduction in the wearing down of the equipment for comminution and conformation (extruder). Moreover, high plasticity is associated with bodies with greater mechanical strength (Monterio and Vieira, 2004). Fig. 10 shows the position of these clays on the Holtz and Kovacs Diagram (Holtz

and Kovacs, 1981). The position of the MC and the KC on the diagram shows that the samples are presented between illitic and montmorillonitic domains. However, the MC is quite near the illite field, possibly due to kaolinite contents coherent with the XRD results. On the other hand, the KC is quite near the montmorillonite field.

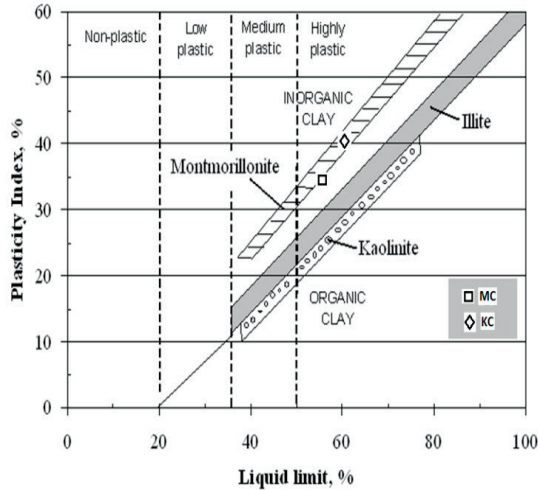


Figure 9. Location of the MC and the KC samples on the Casagrande chart

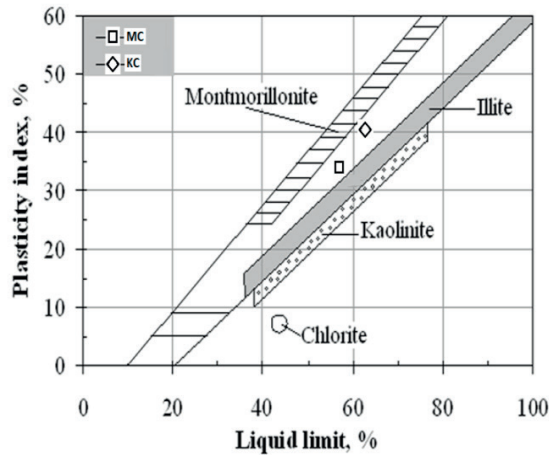


Figure 10. Position of the MC and the KC on the Holtz and Kovacs diagram

**2.6. Drying Sensitivity Measurement**

The plot of drying shrinkage vs. loss of moisture content (Bigot’s curve) of the clay bodies is shown in Fig.11. The initial moisture ( $M_i$ ), the critical moisture at which the linear drying shrinkage finishes ( $M_c$ ), drying shrinkage (DS) and Drying Sensitivity Index (DSI) of all clay mixtures are

shown in Table 3. The theory and modeling for drying of ceramic bodies have been the subject of many studies (Aungatichart and Wada, 2009; Ford, 1986; Konig, 1998; Scherer, 1990). The relevant literature on drying divide a drying process into (I) “constant rate period” with initial weight loss and major shrinkage, and (II) “declining rate period” with successive weight loss and minor shrinkage. The shrinkage process can lead to the occurrence of the drying crack of the ceramic bodies. Drying crack is also related to the term “drying sensitivity” (Aungatichart and Wada, 2009). As seen from Fig. 11, at the end of the constant rate period the MC lost 12.04% moisture whereas the KC lost 15.06%. It is concluded from Table 3 that the KC has the less DSI (0.75) value than the MC (0.84). The high DSI value reflects the high stress in the ceramic body that is dried quickly or unevenly and as a result, this body is prone to break during the drying process (Aungatichart and Wada, 2009). According to obtained these results, it can be said that the MC is more sensitive to drying process than the KC. Similarly, it was observed at the end of the drying process that the MC had more drying cracks than that of the KC had.

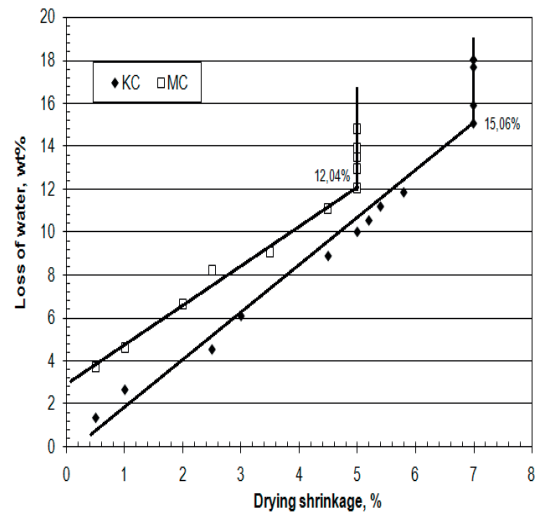


Figure 11. Relationship between drying shrinkage and loss of moisture content of the clay samples

**3. CONCLUSIONS**

The clays from Menemen and Kinik region, Turkey were characterized by chemical, mineralogical and thermal analyses. As concluding remarks, the following aspects related to the characterization and industrial application of two clays can be summarized:

1. It appears that from the mineralogical point of view, the main phase present in Menemen Clay (MC) was muscovite and kaolinite at an amount of about 51% and containing a substantial amount of SiO<sub>2</sub> and albite and calcite as main impurities. The ceramic materials from Kınık region (KC) consisted mostly of clinocllore and muscovite clay minerals at an amount of 41% with a high SiO<sub>2</sub> content (about 50%) as well as a low amount of alkaline oxides. The results from the chemical analyses of the raw clays show that the most important are Al<sub>2</sub>O<sub>3</sub> and SiO<sub>2</sub> since they have a decisive influence on the refractoriness and strength of the final ceramic product.

2. The samples basically consist of a finely grained material. The MC consists of <2µm material around 46% whereas the KC 40%. As a consequence of this, the MC has a higher plastic limit than the KC. Higher proportions of finer particles and higher content of alkaline oxide especially for the MC favored vitrification due to good compaction of samples during firing. This has a positive effect on the firing strength of the MC clay samples. The firing strength value of the MC was 1.1 times greater than that of the KC, whereas water absorption value of the MC was 1.3 times less than the KC.

3. Concerning the technological parameters of fired bodies, the MC had higher firing and total shrinkage values than the KC due to the presence of more quartz in the KC and more clay minerals in the MC.

4. The relationship between water absorption, firing shrinkage and strength as a function of the firing temperature was examined for both clay samples, and above 950°C, water absorption was decreased and firing strength was increased distinctly with rising temperature of firing. The higher percentage of alkaline flux for the MC contributes achieving a low-level of water absorption above 950°C.

5. It was concluded from the drying sensitivity test that the KC has less DSI value of 0.75 than the MC (0.84). Since the MC is more sensitive to the drying process, the MC led to the occurrence of more drying cracks than the KC.

6. Characterization of Kınık Clay and comparison of Menemen and Kınık clay deposits have not been studied widely before. It is expected that the present investigation will help to improve the knowledge of both deposits. Investigations are still continuing on this important clay deposits for its exploitation for sustainable development.

## REFERENCES

- Ancey, C., 2007. Plasticity and Geophysical Flows: A Review. *Journal of Non-Newtonian Fluid Mechanics* 142 (1-3), 4-35.
- Atanasov, A., 2005. Drying Properties of a Ceramic Mass Resistible to Aggressive Environment. *Journal of the University of Chemical Technology and Metallurgy*, 40 (4), 311–314.
- Aungatichart, P., Wada, S. 2009. Correlation Between Bigot and Ratzenberger Drying Sensitivity Indices of Red Clay from Ratchaburi Province (Thailand). *Applied Clay Science*, 43, 182–185.
- Baccour, H., Medhioub, M., Jamoussi, F., Mhiri, T., Daoud, A., 2008. Mineralogical Evaluation and Industrial Applications of the Triassic Clay Deposits, Southern Tunisia. *Materials Characterization*, 59, 1613-1622.
- Baccour, H., Medhioub, M., Jamoussi, F., Mhiri, T., 2009. Influence of Firing Temperature on the Ceramic Properties of Triassic Clays from Tunisia. *J. Materials Processing Technology*, 209 (6), 2812-2817.
- Bergaya, F., Lagaly, G., 2006. General Introduction: Clays, Clay Minerals and Clay Science, in *Handbook of Clay Science* edited by F. Bergaya, B.K.G. Theng, G. Lagaly, Published by Elsevier, p.5-6.
- Can, M.M., Ozcan, S., Ceylan, A., Firat, T., 2010. Effect of Milling Time on the Synthesis of Magnetite Nanoparticles by Wet Milling. *Materials Science and Engineering B*. 172, 72-75.
- Carretero, M.I., Dondi, M., Fabbri, B., Raimondo, M., 2002. The Influence of Shaping and Firing Technology on Ceramic Properties of Calcareous and Non-Calcareous Illitic–Chloritic Clays. *Applied Clay Science*, 20, 301– 306.
- Casagrande, A., 1947. Plasticity Chart for the Classification of Cohesive Soils. *Trans. Am. Soc. Civ. Eng.* 783-811.
- Celik, H., 2010. Technological Characterization and Industrial Application of Two Turkish Clays for the Ceramic Industry. *Applied Clay Science*, 50, 245-254.
- Celik, H., 2015. Recycling of Boron Waste to Develop Ceramic Wall Tile in Turkey. *Transactions of The Indian Ceramic Society*, 74 (2), 108-116.
- Colak, M., Aksu, G., 2001. Ceramic Raw Materials of Menemen (İzmir) Their Mineralogical and Chemical Properties. *Proceedings Book of 10th National Clay Symposium, Konya*, 228-234 (in Turkish).
- Diels, K., Jaeckel, R., 2013. *Leybold Vacuum Handbook*. Published by Pergamon Press Ltd., p.185.

- Fisher, P., 1984. Some Comments on the Color of Fired Clays. *Ziegelindustrie International*, 37, 475-483.
- Ford, R.W., 1986. *Ceramics Drying*. First ed. Pergamon, Oxford.
- Harvey, C.C., Murray, H.H. 2006. *Clays: An Overview*, in *Industrial Minerals & Rocks: Commodities, Markets, and Uses 7th ed.*, edited by J. E. Kogel, et al., Published by Society for Mining, Metallurgy, and Exploration. pp.335-336.
- Holtz, R.D., Kovacs, W.D., 1981. Kansas Geotechnical Survey, Current Research in Earth Science. *Bulletin* 244, part 3, The Relationship Between Geology and Landslide Hazards of Atchison, Kansas and Vicinity.
- Konig, R., 1998. *Ceramic Drying*. First ed. Novokeram, Krumbach.
- Kreimeyer, R., 1987. Some Notes on the Firing Color of Clay Bricks. *Applied Clay Science*, 2, 175-183.
- Kurama, S., Kara, A., Kurama, H., 2007. Investigation of Borax Waste Behaviour in Tile Production. *Journal of the European Ceramic Society*, 27 (2-3), 1715–1720.
- Lutterotti L., 2010. MAUD WEB, version 1.9. <http://www.ing.unitn.it/~luttero/maud>.
- Mahmoudi, S., Srasra, E., Zargouni, F., 2008. The Use of Tunisian Barremian Clay in the Traditional Ceramic Industry: Optimization of Ceramic Properties. *Applied Clay Science*, 42, 125-129.
- Modesto, de C.O., Bernardin, A.M., 2008. Determination of Clay Plasticity: Indentation Method versus Pfefferkorn Method. *Applied Clay Science*, 40, 15-19.
- Monterio, S.N., Vieira, C.M.F., 2004. Influence of Firing Temperature on the Ceramic Properties of Clays from Campos Dos Goytacazes, Brazil. *Applied Clay Science*, 27, 229-234.
- Ozkan, I., 2015. Densification Behavior of Red Firing Menemen Clay. *Journal of the Australian Ceramic Society*. 51, 36–39.
- Peters, J.F., 1991. Determination of Undrained Shear Strength of Low Plasticity Clays. *International Journal of Rock Mechanics and Mining Science and Geomechanics Abstracts*, 28 (1), 13.
- Ratzenberger, H., 1986a. Causes and Methods of Determining the Drying Sensitivity of Raw Materials for Structural Ceramics and Heavy Clay Products. *Ziegelindustrie International* 10, 535–540.
- Ratzenberger, H., 1986b. Possibilities for Reducing the Drying Sensitivity of Ceramic Raw Materials. *Ziegelindustrie International*, 11, 594–599.
- Ratzenberger, H., 1990. An Accelerated Method for the Determination of Drying Sensitivity. *Ziegelindustrie International*, 6, 348–354.
- Reinholz, S.Ch., 1987. Natural Drying Sensitivity of Clay Ceramic Raw Materials and Bodies Causes and Restriction through Additives. *Interbrick*. 3 (6), 23–27.
- Schneider, H.E., Hanke, W., 1996. Determination of the Drying Crack Sensitivity of Structural Ceramics and Heavy Clay Raw Materials. *Ziegelindustrie International*, 7–8, 468–480.
- Scherer, G.W., 1990. Theory of Drying. *Journal of the American Ceramic Society* 73, 3–14.
- Singer, F., Singer, S.S., 1963. *Industrial Ceramics*. Chapman and Hall Ltd, London. 99-100.
- Souza, G.P., Sanchez, R., de Holanda, J.N.F., 2002. Characteristics and Physical-Mechanical Properties of Fired Kaolinitic Materials. *Ceramica*. 48 (306), 102-107.
- TS EN ISO 10545-3, 1995. *Ceramic Tiles—Part 3: Determination Of Water Absorption, Apparent Porosity, Apparent Relative Density and Bulk Density*. Turkish Standards Institution.
- TS EN ISO 10545-4, 1995. *Ceramic Tiles—Part 4: Determination Of Modulus Of Rapture and Breaking Strength*. Turkish Standards Institution.